Title

Ionospheric ambipolar electric fields of Mars and Venus: Comparisons between theoretical predictions and direct observations of the electric potential drop.

Journal

Geophysical Research Letters, 46(3)

ISSN

0094-8276

Authors

Collinson, Glyn

Glocer, Alex

Xu, Shaosui

et al.

Publication Date

2019-02-16

DOI

10.1029/2018GL080597

Peer reviewed

Published in final edited form as:
Geophys Res Lett. 2019 February 16; 46(3): 1168–1176. doi:10.1029/2018GL080597.

Ionospheric ambipolar electric fields of Mars and Venus: Comparisons between theoretical predictions and direct observations of the electric potential drop

Glyn Collinson[1,2,3], **Alex Glocer**[1], **Shaosui Xu**[3], **David Mitchell**[3], **Rudy A Frahm**[4], **Joseph Grebowsky**[1], **Laila Andersson**[5], **Bruce Jakosky**[5]

[1]NASA Goddard Spaceflight Center, Greenbelt, Maryland, USA.

[2]Institute for Astrophysics and Computational Sciences, The Catholic University of America, Washington, District of Columbia, USA

[3]Space Sciences Laboratory, University of California, Berkeley, California, USA

[4]Southwest Research Institute, San Antonio, Texas, USA

[5]Laboratory For Atmospheric and Space Physics, Boulder, Colorado, USA

Abstract

We test the hypothesis that their dominant driver of a planetary ambipolar electric field is the ionospheric electron pressure gradient (∇P_e). The ionospheres of Venus and Mars are mapped using Langmuir probe measurements from NASA's *Pioneer Venus Orbiter (PVO)* and *Mars Atmosphere and Volatile Evolution (MAVEN)* missions. We then determine the component of the ionospheric potential drop that can be explained by the electron pressure gradient drop along a simple draped field line. At Mars, this calculation is consistent with the mean potential drops measured statistically by MAVEN. However, at Venus, contrary to our current understanding, the thermal electron pressure gradient alone cannot explain Venus' strong ambipolar field. These results strongly motivate a return to Venus with a comprehensive plasmas and fields package, similar to that on MAVEN, to investigate the physics of atmospheric escape at Earth's closest analog.

1. Introduction

One mechanism thought to play a key role in ion outflow and escape at all planets is an ionospheric "ambipolar" electric field (also sometimes referred to as a "polarization" electric field). It is an energy field generated by the planetary ionosphere itself, and is as much an intrinsic property of a planet as the depth of its gravity well or the strength (or absence) of a global magnetic dynamo field. The potential drop that results from this electric field assists terrestrial atmospheric escape [Moore et al., 1997] since it reduces the potential barrier required for heavier ions (such as O+) to escape and accelerates light ions (such as H+) to escape velocity. This potential drop is critical to the formation of Earths "polar wind" which

Corresponding author: Glyn Collinson, Heliophysics Science Division, NASA Goddard Space Flight Center, Greenbelt, MD, USA. (glyn.a.collinson@nasa.gov).

flows outward along open magnetic fields above our polar caps [Banks and Holzer, 1968]. Although vital to our understanding of atmospheric evolution, this field is extremely challenging to measure given its small magnitude. However, several recent studies have succeeded in measuring the total electric potential drop associated with ambipolar electric fields in the ionospheres of Mars and Venus.

At Mars, a preliminary pilot study by Collinson et al. [2015] shortly after orbital insertion of NASA's *Mars Atmosphere and Volatile Evolution (MAVEN)* spacecraft put an upper limit of $< \pm 2\,V$ on the ionospheric potential drop. Recently, Xu et al. [2018] used the comprehensive particles and fields package on *MAVEN* to statistically map the global distribution of field-aligned potentials at Mars, finding them to have Gaussian-like distributions, with mean values ranging from 0 to −1.5V. Overall, below 800km, Xu et al. [2018] found that the potential drop was near zero at ~180km, increased to between $-0.4\,V$ and −0.7V at $\approx 220\,km$, and then remained quasi-constant above.

At Venus, Collinson et al. [2016] performed a preliminary survey of ionospheric ambipolar potentials from 2 years of data from the ESA *Venus Express* mission (2006–2014) [Svedhem et al., 2007]. Whereas the comprehensive suite of sensors on *MAVEN* permits constant monitoring of planetary potentials at 1s cadence, limitations of the skeleton instrument package aboard the *Venus Express* severely limited the window of observations to only 14 measurements on six orbits. However, contrary to all expectations, the potential drop in Venus' ionosphere was found to be $-9.9\,V \pm 1.1\,V$, sufficient to accelerate heavy ions such as O^+ directly to escape velocity. Although not a statistical sample, the potential drop was found to be consistently ≈10V from orbit to orbit, and remained steady for periods of up to five consecutive minutes.

Now that ambipolar potential drops have been measured at two planets, we may investigate the fundamental physics that drives them. Specifically, in this study we investigate the hypothesis that the dominant driver of ambipolar fields is the change in electron pressure (P_e) with distance (s) along the open magnetic field line [Schunk and Nagy, 2004; Varney et al., 2014]. In this paper, the physics behind the formation of ambipolar fields is described in section 2. In section 3 we map the ionospheres of Venus and Mars, calculate the electron pressure gradient along a simple draped interplanetary magnetic field line, and calculate the total resultant potential drop expected. Finally, in section 4 we discuss our results.

2. What generates an ionospheric ambipolar field?

At Earth's magnetic poles, open magnetic field lines provide a pathway for ionospheric plasma to escape into the solar wind. At Venus and Mars, which have no magnetic dynamo, open field lines may be found globally (with the exception of in Mars' crustal remnant fields [Acuña et al., 1998]). However, in order to escape from the ionosphere, a particle must first overcome the planetary gravitational potential. It is much harder for an ion to overcome gravity than an electron, which is three to four orders of magnitude lighter. Thus, in the absence of ions, ionospheric electrons would easily escape under their own thermal pressure gradient (∇P_e). However, due to quasi-neutrality, the electrons (with density n_e, and charge

e) are coupled to the ions, and an ambipolar field-aligned electric potential forms to resist their separation.

In order to understand what controls the strength of ambipolar field at any planet, we must consider the physics behind what is restraining the electrons as they "push" outwards (as in Figure 1). Equation 1 describes these processes, and the resulting generation of an ionospheric parallel ambipolar electric field ($E_\parallel$)

$$E_\parallel = -\frac{1}{en_e}\left[\underbrace{\frac{\partial P_e}{\partial s}}_{\mathbf{A}.} + \underbrace{\frac{\partial}{\partial s}\rho_e u_e^2 + \frac{B'}{B}\rho_e u_e^2}_{\mathbf{B}.} - \underbrace{\frac{\delta M_e}{\delta t}}_{\mathbf{C}.}\right] \quad (1)$$

This equation describes the Ohm's law and is consistent with the $E_\parallel$ derived by Gombosi and Nagy [1989], Liemohn et al. [1997], and Varney et al. [2014] from the electron momentum equation assuming a scalar pressure, a steady state approximatation for the superthermal electrons, and negelecting terms proportional to m_e/m_i. In plain english, however, Equation 1 can be broken down into three basic physical processes. (Note however that Equation 1 does not include the effect of pressure tensors or exotic processes such as double layers.)

A. Electron pressure gradient:

At Earth, the dominant term in Equation 1 is often presumed to be the change in electron pressure (P_e) with distance (s) along the magnetic field line [Varney et al., 2014] since the other two terms involve the electron mass (m_e), which is very small when compared to the mass of the ions (m_i). Equation 1 may then be simplified to a form directly measurable by Langmuir Probe:

$$E_\parallel \approx -\frac{1}{en_e}\frac{\partial P_e}{\partial s} \quad (2)$$

B. Electron inertia:

The faster the change in electron momentum flux (e.g. mass density (ρ_e) times the square of the electron bulk velocity (u_e)) along the field line, the stronger the electric field required to restrain the electrons to maintain quazi-neutrality. This term also includes a correction for the adiabatic magnetic effects resulting from any change in magnetic field strength between the source in the ionosphere (B) and the spacecraft (B').

C. Collisional processes:

The final term incorporates the contribution due to the change in momentum of electrons due to collisional processes. This term can be expanded into three components:

$$\frac{\delta M_e}{\delta t} = C_1 + C_2 + C_3 \quad (3)$$

Where:

$$C_1 = m_e n_e \sum_i \nu_{ei}(u_i - u_e) + m_e n_e \sum_i \nu_{ei}(u_n - u_e) \quad (4)$$

This represents the change in momentum of the electron bulk flow due to collisions with ions and neutrals (flowing at different bulk velocities u_i, u_n). The strength of this term is regulated by the magnitude of the velocity difference as well as collision frequency between electrons and ions (ν_{ei}) and electrons and neutrals (ν_{en}). This form of C_1 is known as Burgers linear approximation of the collisional terms for the five-moment equations [Burgers, 1969]. This approximation by itself may not be sufficient for all conditions (especially when the velocity difference between electrons and ions/neutrals is large). In particular, this approximation does not account for the skew in the electron distribution function due to a heat flux. Thus there exist further corrections to the collisional term, which expand their applicability. These are:

$$C_2 \approx -\frac{m_e}{k_B T_e}\left(\frac{3}{5}\sum_i \nu_{ei} + \sum_n \nu_{en} z_{en}\right)\kappa_e \frac{\partial T_e}{\partial s} \quad (5)$$

Where κ_e is the electron thermal conductivity. Equation 5 represents this additional term, taken from Burgers linear approximation for the eight-moment equations as presented by Schunk and Nagy [2004] and Varney et al. [2014]. The heat flux of the electrons introduces a skew in the electron distrbution which changes the momentum transfered between the electrons and ions/neutrals. Varney et al. [2014] argues this term is largely approximated by equation 5, which is known as the “thermal diffusion effect”.

There is one final contribution to the collisional term which is the collisional dragging of thermal electrons by hotter superthermal electrons (C_3). When superthermal electrons stream through the thermal electrons, the Coulomb collisions between the two populations result in a net transfer of momentum. This imparts extra energy to the thermal electrons, and thus an additional electric field is required to restrain the thermal electrons [Varney et al., 2014]. We do not write the analytical expression for C_3 here (for sake of brevity), but it is readly found in [Liemohn et al., 1997, eq. 8] or [Varney et al., 2014, eq. B9].

Superthermal Electrons: Broadly speaking, the more energetic the electrons, the stronger the electric field must be to restrain them. “Superthermal” (1 – 70 eV) photoelectrons, generated by photoionization of the atmosphere, play an especially potent role in generating this field [Lemaire, 1972] even though they make up a small fraction of the total electron population (< 0.1% at Earth) [Khazanov et al., 1997]. This is because while not explicitly called out in equation 1, excepting the collisional dragging, they enhance every term. Collinson et al. [2016] thus hypothesized that Venus’ relatively strong ambipolar field may be a result of greater relative admixtures of photoelectrons at Venus than at Earth. However, this hypothesis has yet to be investigated.

In this paper we examine the hypothesis that planetary ambipolar fields may be approximated by only considering the electron pressure gradient along the open field line (equation 2). To do this, we obtain a first order approximation of the average field-aligned

electron pressure gradient at Mars and Venus. We then calculate the resulting total electric potential drop and compare with experimental observations at Venus and Mars.

3. Examining the role of electron pressure gradient in the formation of ambipolar fields

To test equation 2, we will **1.)** Map the thermal electron pressure in the ionospheres of Venus and Mars using in-situ Langmuir Probe measurements; **2.)** Measure the thermal electron pressure at numerous points along a simplified draped interplanetary magnetic field line model; **3.)** Fit a function to these data, and by differentiating, find the gradient and thus the electric field; and **4.)** Integrate $E_{\parallel}$ along the field line to calculate the total potential drop (Θ), which may be directly compared with the ionospheric potentials recently measured at Venus [Collinson et al., 2016] and Mars [Xu et al., 2018].

3.1. Mapping the ionospheres of Venus and Mars

The first step in calculating the contribution of thermal electron pressure towards the ambipolar electric field ($E_{\parallel}$, Equation 2) is to map thermal electron pressure in the ionospheres of Venus and Mars. The thermal pressure of ionospheric electrons may be found simply by applying the ideal gas law (equation 6, where k_B is Boltzmann's constant):

$$P_e = n_e T_e k_B \tag{6}$$

The density (n_e) and temperature (T_e) of electrons in a planetary ionosphere may be directly measured *in-situ* using a Langmuir probe, which have now been flown to both Venus and Mars. At Venus, NASA's *Pioneer Venus Orbiter* (PVO) carried the Orbiter Electron Temperature Probe (OETP) instrument [Brace et al., 1979; Krehbiel et al., 1980], which measured n_e and T_e throughout the Venusian ionosphere between 1978 and 1992. At Mars, NASA's *Mars Atmosphere and Volatile EvolutioN* (MAVEN) mission carries the Langmuir Probe and Waves (LPW) instrument [Andersson et al., 2015], which has been operating at Mars since 2014.

Figure 2 shows maps of the ionospheres of Venus and Mars. Fig 2A,B show collected LPW density and temperature observations at Mars from a period covering the first 5000 orbits of MAVEN (September 2014 → April 2017). LPW data have been limited to the northern Martian hemisphere to reduce any effects due to remnant crustal magnetic anomalies, which are found mostly in the southern hemisphere [Connerney et al., 1999]. Fig 2D,E show maps of the electron density and temperature from the entire PVO mission. The x-axis of each map shows Solar Zenith Angle (SZA), with 0° being noon and 180° midnight. The y-axis of each map shows altitude in km (logarithmic plot). n_e and T_e were binned by SZA and Altitude, and a geometric mean taken in each SZA/altitude bin. The resulting global maps of n_e and T_e were multiplied together with k_b to create maps of ionospheric pressure (P_e) at Mars (2C) and Venus (2F). White areas denote a lack of coverage.

With the two planets side-by-side, Venus' thicker ionosphere is immediately apparent, with higher densities at higher altitudes than at Mars. Both ionospheres fade away across the

terminator (90° SZA), with much over an order of magnitude higher densities and pressures on the dayside (0° → 90° SZA) than the nightside (90° → 180° SZA).

3.2. Measuring the electron pressure along a simplified draped interplanetary magnetic field line model

The second step in solving for $E_{\parallel}$ (Eqn. 2) is to determine electron pressure (P_e) with distance (s) along a magnetic field line. To do this, we must assume a magnetic field geometry. To obtain a rough first approximation of the average field-aligned electron pressure gradient at Mars and Venus, we shall assume a highly simplified model of a draped interplanetary magnetic field (IMF) line, which assumes that the field line wraps around the planet at a constant altitude from the sub-solar point to the terminator, and then drapes off in a straight line going down the tail (e.g. Fig. 1, red line). Let us also ignore the magnetic crustal anomalies at Mars [Acuña et al., 1998; Connerney et al., 1999], since these are highly complex and not present at Venus. We acknowledge that this field-line geometry is a highly over-simplistic assumption, but is adequate for a first-order approximation, and will taken will be taken into account when drawing conclusions.

This simplified field-line geometry (identical at both planets) is shown on Figure 2 as a red line at a constant altitude (160 km) between 0° → 90° SZA, and then increasing almost linearly in altitude after crossing the terminator. This constant altitude of 160 km has been chosen as being the lowest altitude for which we have consistent global coverage of observations at both Venus and Mars. While slightly above the main ionospheric density peak (150 km at Venus [Brace and Kliore, 1991], 120 → 160 km [Hantsch and Bauer, 1009]), this nevertheless still allows us to capture the majority of the ionospheric density/ pressure gradient, and is thus adequate for a first order investigation of equation 2.

Figure 3 shows densities, temperatures, and pressures extracted from our ionospheric maps (Fig 2) along this simplified draped field-line model. *PVO-OETP* measurements at Venus are shown in blue-grey, and *MAVEN-LPW* at Mars are shown in maroon. Left-hand panels (Fig. 3A-D) again show variations with Solar Zenith Angle (SZA in degrees), right-hand panels (Fig. 3E-H) show variations with altitude (km). The distribution of P_e along this simplified IMF field line is shown in Figures 3C,G. There is substantial variability in *MAVEN-LPW* measurements at higher altitudes, which is due to the variability of the Martian nightside ionosphere.

3.3. Determining the gradient of electron pressure and the resulting ambipolar electric field

To calculate $E_{\parallel}$ according to Equation 2, we must differentiate the electron pressure with respect to distance along the field line. Due to the variability in measurements of P_e, we choose to first fit a function to data, and then perform the final steps of analysis with this line of best fit. At Venus, there already exists a sophisticated polynomial model of *PVO-OETP* data by Theis et al. [1980], which closely fits to the observed drop-off in electron pressure with SZA and altitude (Fig. 3C,G). At Mars, we fit *MAVEN-LPW* observations to the polynomial below in Equation 7 (where A = −0.8, B = 37.0, C = 6.8, D = −10.2).

$$P_e(alt) = A \tanh(B(alt - C)) + D \quad (7)$$

We then calculate the distribution of electric field along the simplified IMF field line using Equation 2 (Fig. 3D,H). According to this calculation, Mars generates the strongest instantaneous electric field, peaking at $\approx 1 \mu V/m$ at an altitude of $200 km$ (just above the exobase). This calculation predicts Venus' ambipolar electric field to peak at $\approx 0.4 \mu V/m$ at an altitude of $\approx 220 km$.

3.4. Comparing the calculated total potential drop with observations

Finally, we may integrate the electric field (Fig. 3D,H) to calculate the total electric potential drop along the field line ($\Theta_{\partial Pe/\partial s}$), which may be directly compared to the new observations at Venus and Mars. Performing such an integration, we find that our electron pressure gradient calculation (Eqn. 2) predicts a total potential drop of $\Theta_{\partial Pe/\partial s} = -0.7V$ at Mars, and $\Theta_{\partial Pe/\partial s} = -0.9V$ at Venus.

4. Discussion and conclusions

In calculating the ambipolar electric field (and associated potential drop) at Mars and Venus, several assumptions have been made: (1) The calculation of electron pressure gradient is based on a global statistical average of the ionosphere, whereas in reality planetary ionospheres are far more complex and turbulent; (2) The magnetic field-line geometry assumed is intentionally over-simplistic. With these assumptions in mind, we shall now examine the hypothesis that $E_\parallel$ may be approximated by the electron pressure gradient (Equation 2) by comparing the predicted total potential drop ($\Theta_{\partial Pe/\partial s}$) with recent direct measurements at Mars (Θ_{Mars}) and Venus (Θ_{Venus}).

At Mars the theoretical total electric potential drop estimated using *Mars Atmosphere and Volatile EvolutioN (MAVEN)* Langmuir Probe and Wave (LPW) data ($\Theta_{\partial Pe/\partial s} = 0.7V$) agrees very well with the recent statistical *MAVEN* studies of direct measurements of Θ_{Mars} by Xu et al. [2018]. Using measurements by the *MAVEN* SWEA and STATIC instruments, Xu et al. [2018] created global maps of the total electric potential drop between *MAVEN* and the Martian ionosphere, finding potentials with mean values that range between $0 V < \Theta_{Mars} < -1.5 V$. The mean total potential drop reported by Xu et al. [2018] (between −0.4 V and −0.7 V) are consistent with −0.7 V mean calculated from ∇P_e, and also peaked at a similar altitude ($\approx 220 km$). We thus find that, to the first order, Martian ionospheric ambipolar fields are consistent with what would be expected to result from the gradient of the thermal electron pressure along the magnetic field (Eqn 2).

At Venus, however, the total electric potential drop calculated using the *Pioneer Venus Orbiter (PVO)* Orbiter Electron Temperature Probe (OETP) ($\Theta_{\partial Pe/\partial s} = -0.9V$) is an order of magnitude weaker than that recently reported by Collinson et al. [2016], who used data from the ESA *Venus Express* spacecraft. Whereas *MAVEN* carries a comprehensive suite of particles and fields instruments and is always capable of measuring Θ_{Mars}, the more skeletal package on *Venus Express* meant that measurements of Θ_{Venus} could only be made very

sporadically: 14 windows of observation over 2 (Earth) years of *Venus Express* data. However, although the electric potential could only be measured occasionally, Collinson et al. [2016] found that (a) any time it was possible to measure an electric potential drop, one was observed, and (b) the magnitude of this drop was very consistent (and stable for minutes at a time), with a mean value of $\Theta_{Venus} = -9.9\,V \pm 1.1\,V$. This is an order of magnitude greater than that predicted by the thermal electron pressure gradient.

We will now briefly speculate as to possible explanations for the significant disparity between theory and observations. Some we are able to immediately discount, whereas others remain credible, requiring further exploration at Venus.

Are the strong Venusian electric potential drops the result of transient enhancements?:

One possible explanation is that perhaps transient phenomena in the turbulent Venusian ionosphere create substantial localized transient enhancements in electron pressure gradient. However, this seems unlikely, since Collinson et al. [2016] reported continuous observations for periods of up to 5 minutes, which is not consistent with a transient phenomena.

Would a more realistic field line draping model enhance the pressure gradient?:

Another possible explanation is the highly over-simplified magnetic field geometry used in the calculation of $\Theta_{\partial Pe/\partial s}$. To investigate this, we varied the draping geometry (not shown), but found that this only varied the total potential drop by a few tenths of a volt, and no magnetic field geometry could produce anything close to the measured value.

Are superthermal electrons enhancing Venus' electric field?:

This study has only considered the effect of the low energy "core" or "thermal" population of electrons ($< 1eV$), which make up > 99% of ionospheric electrons. However, as mentioned previously, planetary ionospheres also contain a small admixture of much hotter "superthermal" electrons, such as "photoelectrons" given off by the photoionization of the neutral thermosphere by solar ultraviolet radiation. Despite being only a small fraction of the total electron population, superthermal electrons may significantly enhance ambipolar fields [Lemaire, 1972; Khazanov et al., 1997]. Collinson et al. [2016] hypothesized that one explanation for Venus' stronger ambipolar electric field is a higher proportion of photoelectrons due to its closer distance to the sun and higher photoionization rates.

Are other terms in Ohm's law contributing at Venus?:

As described in Section 2, there are other terms in Equation 1 that may also contribute to $E_{\parallel}$ and thus the total potential drop. Some terms, such as electron inertia (Equation 1,B.) or the first collisional term, (C_1, Equation 4), are unlikely to be signficant contributors because they depend on the bulk flow velocity which is expected to be small compared to the thermal velocity. However there are two remaining collisional terms that might plausibly enhance the potential drop at Venus.

The "thermal diffusion effect" (C_2, equation 5) has been argued by Varney et al. [2014] to be signficantly important to the calculation of $E_{\parallel}$. They claim that in Earth's ionosphere this effect can contribute as much as 50% as the electron pressure gradient. Therefore, we

evaluated the electron-ion collision component of this term using the *Pioneer Venus Orbiter* OETP data. However, we found that it only contributed $\approx 0.1 mV$ to the total potential drop, and could not explain the $10 V$ drops observed by *Venus Express*. Further evaluation of the thermal diffusion effect (including the electron-neutral collisions) is an ideal subject for future studies.

Finally, superthermal electron collisions with thermal electrons (C_3, Equation 3) may be enhancing the collisional term, and hence the potential drop, at Venus. Escaping photoelectrons interact with the thermal electrons via Coulomb collisions, creating a net transfer of momentum. In essence, the photoelectrons effectively drag the thermal electrons outwards and away from the planet. Thus an additional outwards pointing electric field is required to restrain them [Varney et al., 2014]. Evaluating the overall contribution of superthermal electrons to the ambipolar field is thus another prime target for future data analysis and modeling studies.

Is a full electron pressure tensor required?:

This study assumed the pressure gradient (P_e) to be a scalar, which assumes that the electrons can be described by a maxwellian distribution, where off-diagonal terms in the pressure tensor are zero. In this case, Equation 6 would not accurately describe the electron pressure, and there might be significant additional pressure "hiding out" in the off-diagonal terms of the full electron pressure tensor.

Are all the existing measurements of Venus potential drops outliers?:

Due to the lack of a Langmuir Probe on *Venus Express*, measurements of $\Theta_{\partial Pe/\partial s}$ and Θ_{Venus} had to be made by two separate spacecraft, operating in different phases of the solar cycle. Additionally, this meant that the potential drop below *Venus Express* could not be constantly monitored [Collinson et al., 2016] as with *MAVEN*. Thus we are limited to only a handful of observational windows when a measurement of the potential drop is possible. While the potential measured at Venus during these windows was consistently $-10 V$, it is entirely possible that all these measurements represent only the strongest cases of potential drops at Venus, and that the statistical mean is closer to the expected $-0.9 V$. Therefore, while a substantial difference exists between theory and measurements, we must be cautious in our conclusions due to the paucity of data at Venus.

Finally, the explanation for this apparent disparity may yet prove to be **"none of the above".**

The order of magnitude difference between theoretical predictions and observations of the Venusian ionospheric ambipolar potential strongly motivate future research at Venus, beginning with new theory and modeling studies. Finally, we note that this surprising result is only the latest in a long list of unsolved Venusian mysteries, which strongly motivate a return to Venus to study the fundamental physical processes that govern atmospheric escape and evolution at Earth's closest known analog.

Acknowledgments.

Pioneer Venus Orbiter and *MAVEN* data are available from the NASA Planetary Data System. This work was supported by the *MAVEN* mission, NASA's Solar System Workings Program, NASA's Internal Science Funding Model Ionospheric Outflow work package, and at Southwest Research Institute by NASA contract NASW-00003.

References

Acuña MH, et al. (1998), Magnetic Field and Plasma Observations at Mars: Initial Results of the Mars Global Surveyor Mission, Science, 279, 1676, doi: 10.1126/science.279.5357.1676. [PubMed: 9497279]

Andersson L, Ergun RE, Delory GT, Eriksson A, Westfall J, Reed H, McCauly J, Summers D, and Meyers D. (2015), The Langmuir Probe and Waves (LPW) Instrument for MAVEN, Space Sci. Rev, 195, 173–198, doi:10.1007/s11214-015-0194-3.

Banks PM, and Holzer TE (1968), The polar wind, J. Geophys. Res, 73, 6846–6854, doi:10.1029/JA073i021p06846.

Brace LH, and Kliore AJ (1991), The structure of the Venus ionosphere, Space Sci. Rev, 55, 81–163.

Brace LH, Krehbiel JP, Nagy AF, Donahue TM, McElroy MB, Pedersen A, and Theis RF (1979), Electron temperatures and densities in the Venus ionosphere -Pioneer Venus orbiter electron temperature probe results, Science, 203, 763–765, doi: 10.1126/science.203.4382.763. [PubMed: 17832988]

Burgers JM (1969), Flow equations for composite gases, Academic Press, New York.

Collinson G, et al. (2015), Electric Mars: The first direct measurement of an upper limit for the Martian "polar wind" electric potential, Geophys. Res. Lett, 42, 9128–9134, doi:10.1002/2015GL065084.

Collinson GA, et al. (2016), The electric wind of Venus: A global and persistent "polar wind"-like ambipolar electric field sufficient for the direct escape of heavy ionospheric ions, Geophys. Res. Lett, doi:10.1002/2016GL068327.

Connerney JEP, et al. (1999), Magnetic Lineations in the Ancient Crust of Mars, Science, 284, 794, doi:10.1126/science.284.5415.794. [PubMed: 10221909]

Gombosi TI, and Nagy A. (1989), Time-dependent modeling of field aligned current-generated ion transients in the polar wind, J. Geophys. Res, 94, 359–369.

Hantsch MH, and Bauer SJ (1009), Solar control of the Mars ionosphere, Planet. Space. Sci, 38, 539–542, doi:10.1016/0032-0633(90)90146-H.

Khazanov GV, Liemohn MW, and Moore TE (1997), Photoelectron effects on the self-consistent potential in the collisionless polar wind, J. Geophys. Res, 102, 7509–7522, doi:10.1029/96JA03343.

Krehbiel JP, Brace LH, Theis RF, Cutler JR, Pinkus WH, and Kaplan RB (1980), Pioneer Venus Orbiter Electron Temperature Probe, IEEE Transactions on Geoscience and Remote Sensing, 18, 49–54, doi:10.1109/TGRS.1980.350260.

Lemaire J. (1972), Effect of escaping photoelectrons in a polar exospheric model, Space Research XII, pp. 13–14.

Liemohn MW, Khazanov GV, Moore TE, and Guiter SM (1997), Self-consistent superthermal electron effects on plasmaspheric refilling, J. Geophys. Res, 102, 7523–7536, doi:10.1029/96JA03962.

Moore TE, et al. (1997), High-altitude observations of the polar wind., Science, 277, 349–351.

Schunk RW, and Nagy AF (2004), Ionospheres, 570 pp., Cambridge University Press.

Svedhem H, et al. (2007), Venus Express - The first European mission to Venus, Planetary and Space Science, 55, 1636–1652.

Theis RF, Brace LH, and Mayr HG (1980), Empirical models of the electron temperature and density in the Venus ionosphere, J. Geophys. Res, 85, 7787–7794, doi:10.1029/JA085iA13p07787.

Varney RH, Solomon SC, and Nicolls MJ (2014), Heating of the sunlit polar cap ionosphere by reflected photoelectrons, Journal of Geophysical Research (Space Physics), 119, 8660–8684, doi:10.1002/2013JA019378.

Xu S, Mitchell D, McFadden J, Collinson G, Harada Y, Lillis R, Mazelle C, and Connerney J. (2018), Field-aligned potentials at Mars from MAVEN observations, Geophys. Res. Lett

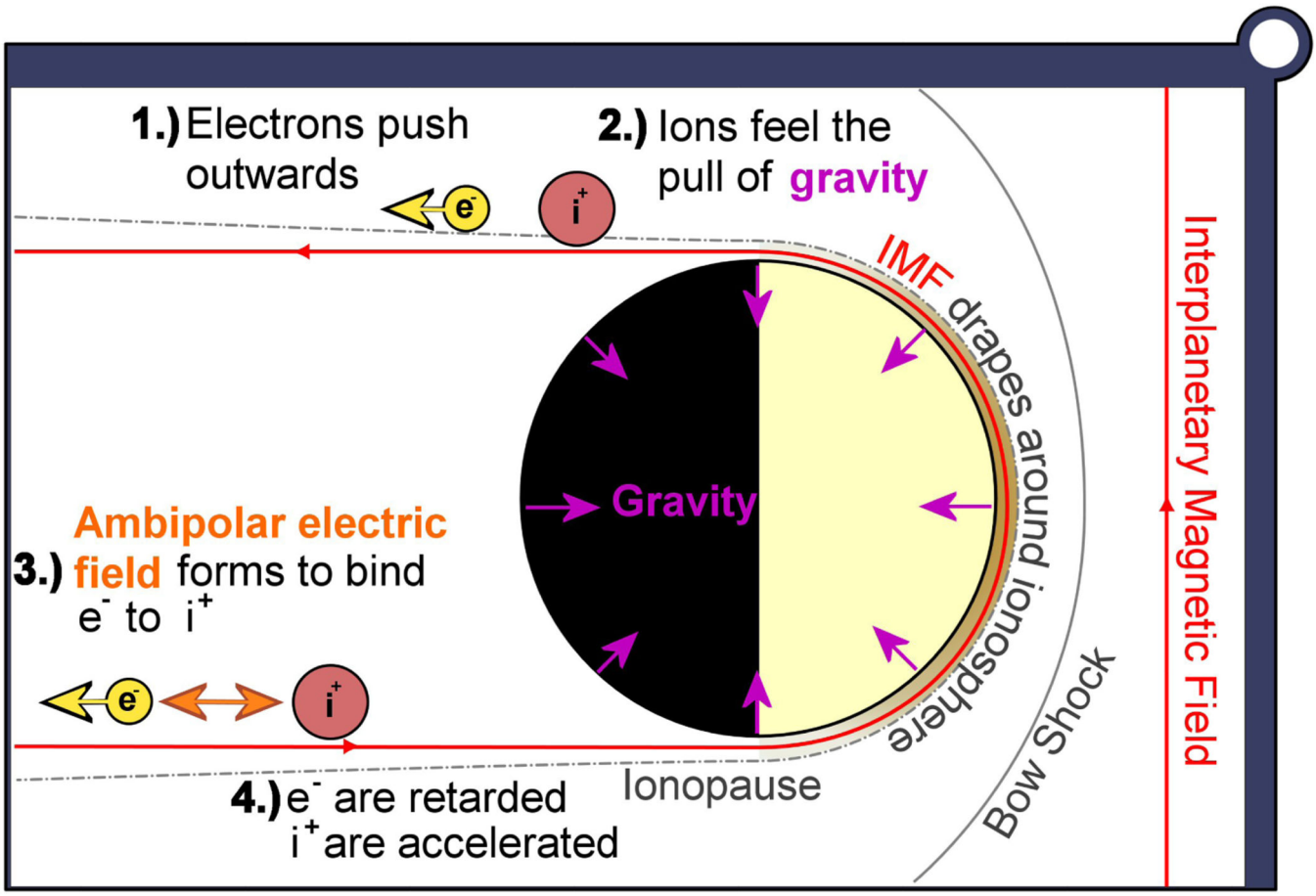

Figure 1.
Sketch showing an induced magnetosphere (such as at Venus and Mars) and the formation of the ambipolar electric field. Reproduced from Collinson et al. [2016].

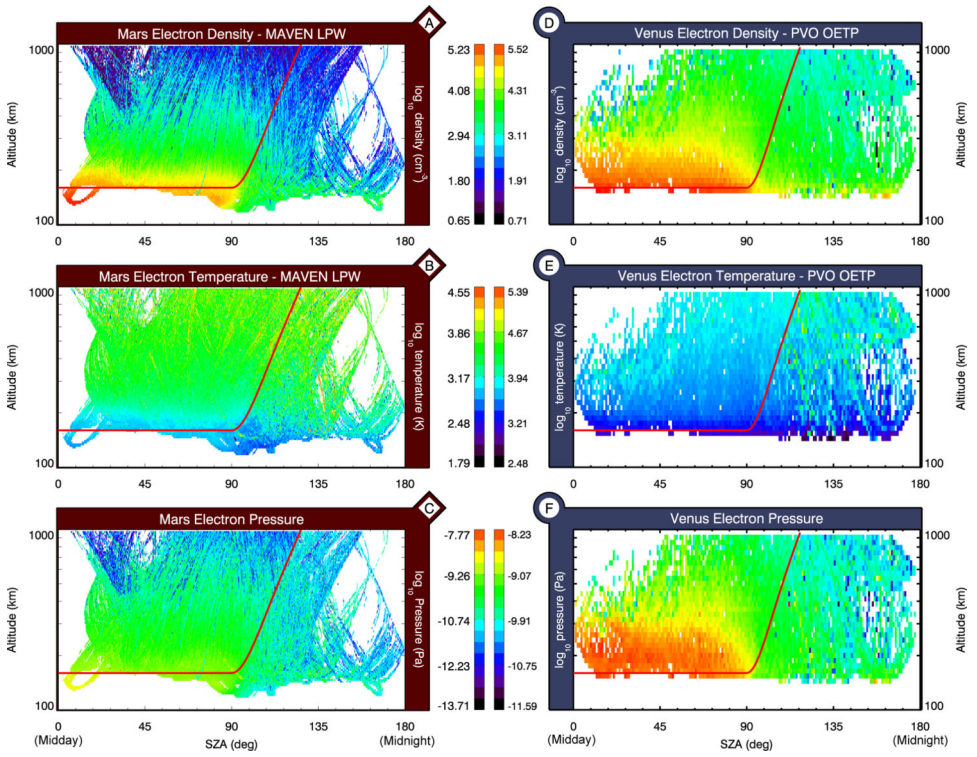

Figure 2.

Panels A-C: Maps of the ionosphere of Mars from combined MAVEN LPW observations. Panels D-F: Maps of the ionosphere of Venus from combined PVO OETP observations. All panels show Solar Zenith Angle (SZA) versus Altitude (log scale), and a red line denotes the path of a draped magnetic field line.

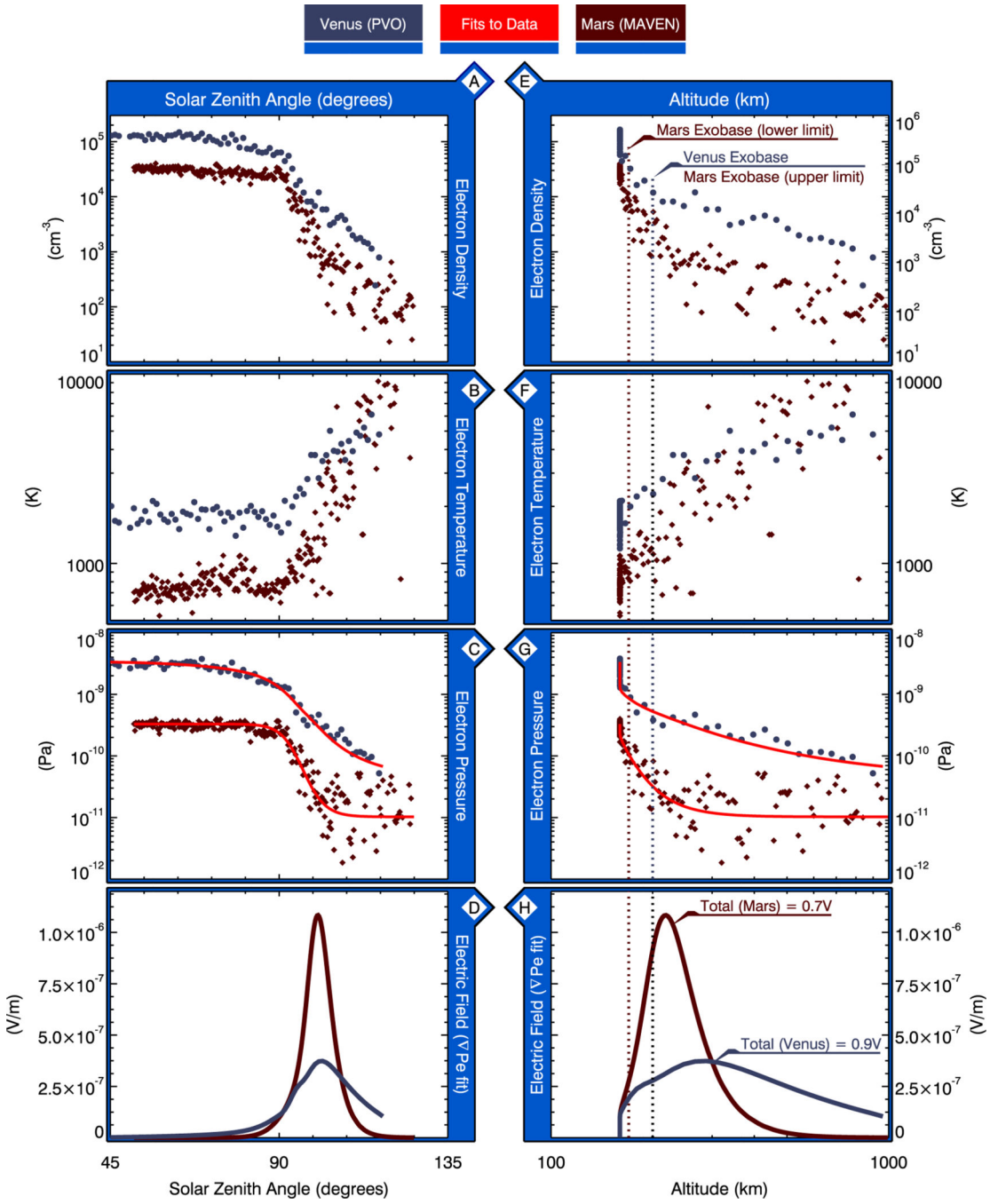

Figure 3.

Evolution of the ionospheric conditions along a draped field line at Mars and Venus. (a-d) Solar zenith angle; (e-h) altitude. Blue dots show Venus (Pioneer Venus Orbiter [PVO]); maroon diamonds show Mars (Mars Atmosphere and Volatile EvolutioN [MAVEN]). Electric fields (d and h) are calculated from fits to electron pressure (red lines, c and g).